Discrete Flow Mapping in coupled two and three dimensional domains: a global interface problem

J Bajars[1], D Chappell[1], T Hartmann[2] and G Tanner[2]

[1] School of Science & Technology, Nottingham Trent University, Nottingham, UK
[2] School of Mathematical Sciences, University of Nottingham, Nottingham, UK

E-mail: janis.bajars@ntu.ac.uk

Abstract. Discrete Flow Mapping (DFM) was recently introduced as a mesh-based high frequency method for modelling structure-borne sound in complex structures comprised of two-dimensional shell and plate subsystems. The method has now been extended to model three-dimensional meshed structures, giving a wider range of applicability and also naturally leading to the question of how to couple the two- and three-dimensional substructures. We consider this problem for the case of a three dimensional interior fluid domain, enclosed by a two dimensional shell/plate system. In Discrete Flow Mapping, the transport of vibrational energy between substructures is typically described via a local interface treatment where wave theory is employed to generate reflection/transmission and mode coupling coefficients. In our case the entire two-dimensional substructure forms a global interface whose radiating properties will depend on both the geometry and the frequency. In this paper we discuss how such a model may be formulated, including both structural radiation and the back-loading of the fluid pressure on the structure.

1. Introduction

Predicting the vibro-acoustic response of complex structures in the high-frequency limit is a major challenge in structural dynamics [1]. *Dynamical Energy Analysis* (DEA) was put forward in Refs. [2, 3, 4] as a robust and relatively widely applicable method, with the ability to interpolate between *Statistical Energy Analysis* (SEA) [5, 6, 7] and full *ray tracing* [8, 9, 10]. DEA is a ray-based energy transport method, where wave energy is propagated along the ray trajectories prescribed by the high-frequency asymptotics of the underlying wave equation. In particular, DEA relaxes one of the key assumptions of SEA requiring well-separated subsystems; this means that the subsystems can be chosen, to some extent, in an arbitrary manner. One particularly convenient choice is to apply DEA directly on finite element meshes [11, 12]. Not only does this remove the considerable modelling effort required in SEA, but the geometric simplicity of typical mesh elements can also be exploited to perform the DEA computations with high efficiency using the so-called *Discrete Flow Mapping* (DFM) approach.

Recently, DFM was extended to three-dimensional tetrahedral meshes in Ref. [13]. In this paper we consider the coupling of two- and three-dimensional DFM for modelling high-frequency energy distributions in fluid-structure interaction problems. In particular, we will present a derivation of the global interface problem given by the coupling of a two-dimensional structural bending wave and a three-dimensional acoustic wave using DFM. We consider a point source excitation of the structure with angular frequency ω, and formulate the coupled wave problem

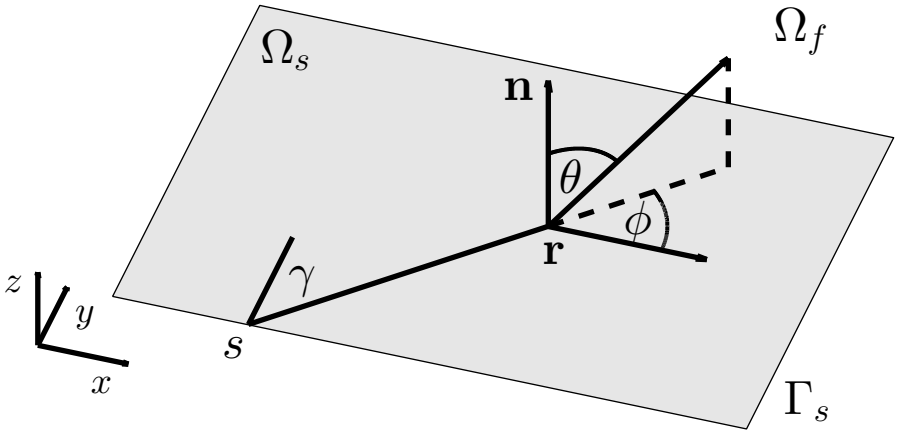

Figure 1. A thin elastic plate Ω_s with boundary Γ_s surrounded by fluid of volume Ω_f. The phase-space boundary density $\rho_A(s, p_s)$ on the structure is prescribed with a position $s \in \Gamma_s$ and a tangential slowness $p_s = \sin(\gamma)/c_b$ for direction $\gamma \in (-\pi/2, \pi/2)$ and bending wave velocity c_b. The volume boundary density $\rho_V(\mathbf{r}, \mathbf{p}_r)$ in the fluid is prescribed with a position $\mathbf{r} \in \Omega_s$ and a tangential slowness $\mathbf{p}_r = [\sin(\theta)/c_0 \quad \phi]^T$ for $(\theta, \phi) \in [0, \pi/2) \times [0, 2\pi)$ and c_0 the speed of sound in the fluid. Note that θ is the angle with respect to the normal vector $\mathbf{n}$ and ϕ is the azimuthal angle in the plate.

in the frequency domain. We derive an energy relationship on the surface of the plate and hypothesize that this relationship must be satisfied by both the two-dimensional (bending wave) and three-dimensional (acoustic wave) energy densities at each point on the plate. In order to extend this coupling to the phase-space densities in DFM, we impose a directionality relationship based on the bending wave properties [14].

The energy relationship on the plate surface will relate the energy density of a bending wave with wavenumber k_b to an acoustic energy density with wavenumber k_0. We note that the transport of both energy densities can be modelled separately by DFM and then coupled together at the parts of the mesh common to both the fluid and the structure. Unfortunately, the energy relationship is not well defined for $k_0 \approx k_b$, and radiation below the critical frequency when $k_b > k_0$ leads to rapidly decaying evanescent waves, which are neglected in our ray-based analysis. Modelling structure-borne sound radiation below the critical frequency would require incorporating wave effects into the model. Nevertheless, in the regime of propagating structural radiation when $k_b < k_0$, a coupled 2D and 3D DFM approach could provide significant insights into the vibro-acoustic properties of complex fluid-structure interaction problems. In particular, the proposed methodology can be applied at frequencies that are too high to be accessible by conventional finite and boundary element methods. In comparison with an SEA treatment, a coupled DFM approach provides a more widely applicable model with a considerable increase in the spatial resolution of the predicted vibroacoustic energy distributions.

2. Problem formulation

In this section we state a general fluid-structure interaction problem for a vibrating thin plate. Consider a flat plate Ω_s with boundary Γ_s coupled to a fluid volume $\Omega_f \subset \mathbb{R}^3$ as depicted in Fig. 1. Without loss of generality we place the plate Ω_s in the xy-plane, that is, we fix $z = 0$. According to the standard Kirchhoff plate theory, the displacement u arising from a time-harmonic bending wave may be coupled to the fluid loading due to a velocity potential ψ

via [15]

$$\frac{Eh^3}{12(1-\nu^2)}\left(\Delta - k_b^2\right)\left(\Delta + k_b^2\right)u = i\rho_f\omega\psi + A\delta(x-x_0)\delta(y-y_0), \qquad (x,y,z)\in\Omega_s, \qquad (1)$$

$$\partial_z\psi = -i\omega u, \qquad (x,y,z)\in\Omega_s, \qquad (2)$$

$$\Delta\psi + k_0^2\psi = 0, \qquad (x,y,z)\in\Omega_f, \qquad (3)$$

where the coupled system is excited by a single frequency ($\omega \gg 1$) point source of magnitude $A \in \mathbb{R}$ at $(x_0, y_0) \in \Omega_s$. Here the bending wavenumber $k_b^4 = 12(1-\nu^2)\rho_s\omega^2/(Eh^2)$, where E is the Young's modulus, ν is the Poisson's ratio of the plate material and h is the thickness. Furthermore, ρ_s and ρ_f are material and fluid densities, respectively, and the acoustic wavenumber $k_0 = \omega/c_0$ is the ratio of the angular frequency ω to the speed of sound c_0 in the fluid. Alternatively, we could have placed the additional point source term on the right hand side of the fluid equation (3). Note that the wave operator on the left of equation (1) has been factorised into dispersive propagating and evanescent decaying parts [16].

Neglecting the contributions due to evanescent waves in equation (1), the left hand sides of the decoupled equations (1) and (3) separately model dispersive and propagating bending waves and (propagating) acoustic waves with wavenumbers k_b and k_0, respectively. As a result, the high-frequency energy distribution due to both waves can be modelled using DFM, with the distinction that the bending wave energy density in the plate is characterised by an area phase space density and the acoustic wave energy density in the fluid is characterised by a volume phase space density. Here we restrict to a scalar wave description of both the fluid and the structural waves; the propagation of multiple plate wave modes (bending, shear and pressure) using DFM is detailed in Ref. [12]. We proceed in the next section by deriving an energy relationship from the coupling equation (2) on the surface of the plate to relate the energies of the structural and acoustic waves.

3. Structure-borne sound: energy and directionality relationships

Following the analysis of [14], we assume a plane wave solution in Ω_s of the form

$$u(x,y) = Ue^{ik_x x}e^{ik_y y}$$

with wavenumber vector (k_x, k_y) such that $k_b^2 = k_x^2 + k_y^2$. In Ω_s, the energy density E_u associated with the wave function u is proportional to the square amplitude, i.e. $E_u = \rho_s h\omega^2|u|^2 = \rho_s h\omega^2 U^2$. Note that E_u describes the energy per area in two-dimensions for a plate of thickness h. In order to match the bending wave solution to the acoustic wave solution with wavenumber k_0 on the surface of the plate, we seek the velocity potential wave solution in the following form:

$$\psi(x,y,z) = \Psi e^{ik_x x}e^{ik_y y}e^{ik_z z}. \qquad (4)$$

The wave function (4) must satisfy the Helmholtz equation (3) and so we have that $k_0^2 = k_x^2 + k_y^2 + k_z^2$, which implies that $k_z = \sqrt{k_0^2 - k_x^2 - k_y^2}$. Note that the acoustic energy density due to the velocity potential ψ in the fluid domain Ω_f is defined as $E_\psi = \rho_f k_0^2|\psi|^2 = \rho_f k_0^2\Psi^2$. Here, the energy density E_ψ defines an energy per volume as usual. From the coupling relation (2) on the surface of plate Ω_s, we obtain the following relationship between the bending and the velocity potential wave amplitudes U and Ψ:

$$\Psi = -\frac{\omega}{k_z}U = -\frac{\omega}{\sqrt{k_0^2 - k_b^2}}U. \qquad (5)$$

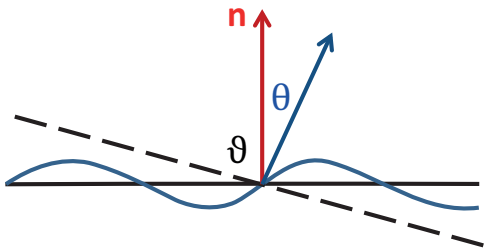

Figure 2. Distinction between the radiation direction angle ϑ and the spherical coordinate system angle $\theta = \pi/2 - \vartheta$.

The wave amplitude relationship (5) for $k_b < k_0$ therefore implies the following relationship on the surface of the plate:

$$\Psi^2 = \frac{\omega^2}{k_0^2 - k_b^2} U^2, \quad k_b < k_0. \tag{6}$$

A direct consequence of (6) is that the energy densities E_u and E_ψ are related via

$$\rho_s h E_\psi = \rho_f \frac{k_0^2}{k_0^2 - k_b^2} E_u, \quad k_b < k_0, \tag{7}$$

and henceforth we will refer to (7) as an energy relationship. If $k_b > k_0$ then $k_z = i\sqrt{k_b^2 - k_0^2}$, leading to evanescent waves in (4) decaying in the normal direction to the plate. We then obtain from the amplitude relationship (5) that

$$\Psi^2 = \frac{\omega^2}{k_b^2 - k_0^2} U^2, \quad k_b > k_0, \tag{8}$$

on the surface of the plate.

Notice that both (6) and (8) are not well defined for $k_b \approx k_0$, when the amplitude of the velocity potential Ψ becomes infinite. In reality, the finite size of the plate and the boundary conditions will prevent the amplitude from blowing up. This leads to a restriction in our modelling and the concept of a critical frequency. The critical frequency f_c is defined when $k_b = k_0$ and we find that

$$f_c = \frac{c_0^2}{2\pi} \sqrt{\frac{12(1-\nu^2)\rho_s}{Eh^2}}. \tag{9}$$

Our analysis is therefore restricted to frequencies above the critical frequency f_c in the propagative wave regime.

Above the critical frequency (9), bending waves radiate sound into Ω_f in a direction $\vartheta \in (0, \pi/2]$ relative to the surface normal vector $\mathbf{n}$ (see Fig. 2). For the purposes of our DFM model it will be convenient to express the angle ϑ in terms of a local upper hemisphere coordinate system for a point $\mathbf{r} \in \Omega_s$ as shown in Fig. 1. In this coordinate system we label the azimuthal angle $\phi \in [0, 2\pi)$ and the longitudinal angle $\theta \in [0, \pi/2)$. The angle θ with respect to normal $\mathbf{n}$ points in the direction of the radiated sound wave such that $\theta = \pi/2 - \vartheta$, see Fig. 2. Then expressing the bending wavenumber vector (k_x, k_y) in terms of the direction (ϑ, ϕ) leads to

$$k_x = k_0 \sin\vartheta \cos\phi, \quad k_y = k_0 \sin\vartheta \sin\phi.$$

We therefore obtain the following directionality relationship:

$$k_b = k_0 \sin\vartheta = k_0 \cos\theta, \quad k_b < k_0. \tag{10}$$

For future reference, we note from (10) that $\sin\theta = \sqrt{1-(k_b/k_0)^2}$. The directionality relationship (10) then leads to an expression for the spherical coordinate system direction angles

$$(\theta, \phi) = (\arccos(k_b/k_0), \phi),$$

for an acoustic wave of wavenumber k_0 radiated due to a bending wave of wavenumber k_b and direction ϕ inside the plate. This observation, together with the energy relationship (7), plays an important role in coupling the 2D and 3D phase space densities of DFM. We proceed in the next section with a brief overview of DFM in two and three dimensions.

4. Brief overview of DEA and DFM

In this section we provide a brief overview of DEA and DFM in two and three dimensions; more details can be found in Refs. [11, 12, 13, 17, 18]. For simplicity, we first consider a single two- or three-dimensional domain Ω with boundary Γ and an initial ray density ρ^0_Γ on Γ, either from interpreting boundary data in terms of an energy density [13] or resulting from interior sources [17]. Then the ray density ρ on the boundary Γ may be transported deterministically along straight-line trajectories (or possibly stochastically [19]) to the next intersection with the boundary by the phase-space boundary integral operator [2]

$$\mathcal{B}[\rho](X) = \int w(Y)\delta(X - \varphi(Y))\rho(Y)\,\mathrm{d}Y. \tag{11}$$

Here $X = (s, p_s)$ for two-dimensional domains and $X = (\mathbf{r}, \mathbf{p}_r)$ in three dimensions; Y is defined analogously. Thus X and Y represent phase-space coordinates on the boundary, that is, s or $\mathbf{r}$ parametrise the boundary of the domain, and p_s or $\mathbf{p}_r$ denote the direction (or slowness vector) component tangential to the boundary at s or $\mathbf{r}$, respectively. The boundary map $\varphi(Y)$ takes a ray with starting position and direction specified by Y and maps it at constant speed along a straight line path to the next intersection with the boundary. At this boundary intersection point the ray is typically assumed to undergo a specular reflection; for multi-domain problems then reflection and transmission are both possible. Note that φ is invertible in convex domains. The weight function w contains absorption factors such as $e^{-\mu L}$, where L is a distance between two boundary intersection points and μ is a parameter specifying the rate of dissipation. The stationary density on the boundary induced by an initial boundary distribution ρ^0_Γ is then obtained using

$$\rho_\Gamma = \sum_{n=0}^{\infty} \mathcal{B}^n[\rho^0_\Gamma] = (I - \mathcal{B})^{-1}[\rho^0_\Gamma], \tag{12}$$

where $\mathcal{B}^n$ contains trajectories undergoing n reflections at the boundary. The energy density distribution in the interior region can subsequently be obtained from the boundary density ρ_Γ by projecting down onto coordinate space.

A generalization to multi-domain (DEA) or meshed structures (DFM) with N sub-domains (or elements) Ω_j, $j = 1, \ldots, N$, is straightforward by introducing a multi-domain boundary map $\varphi_{i,j}$ and a weight function $w_{i,j}$ describing the flow from the boundary of the domain Ω_j to the boundary of the domain Ω_i. Note that $\Omega = \cup_{j=1}^N \Omega_j$ becomes the union of all sub-domains and Γ becomes the union of all sub-domain boundaries, i.e. $\Gamma = \cup_{j=1}^N \partial\Omega_j$. Each sub-domain Ω_j has its own phase-space boundary coordinates. We then define the boundary integral operator $\mathcal{B}_{i,j}$, which transports the phase space density ρ_Γ from the boundary phase-space of Ω_j to the boundary phase-space of Ω_i. If the properties of two neighbouring domains Ω_j and Ω_i are different then, in addition to the dissipative factor, the weight function $w_{i,j}$ will account for the probability of transmission or reflection at the common edge or face in two or three dimensions,

respectively. The operator $\mathcal{B}$ is then constructed from the set of inter-domain operators $\mathcal{B}_{i,j}$ and the stationary density is computed again according to (12).

In the next section we derive a coupling relationship between a 2D (area) phase-space density resulting from the structural bending waves and a 3D (volume) phase-space density resulting from the acoustic waves in the coupled fluid domain.

5. Coupling of the phase space densities in two and three dimensions

Consider a 2D boundary phase-space density $\rho_A(s, p_s)$ and a 3D boundary phase-space density $\rho_V(\mathbf{r}, \mathbf{p}_r)$. The position coordinate s parametrises Γ_s and $p_s = \sin(\gamma)/c_b$ with direction $\gamma \in (-\pi/2, \pi/2)$ and bending wave velocity $c_b = \omega/k_b$. Here γ is the angle between the propagation direction and the normal vector to Γ_s pointing into the domain Ω_s. The 3D volume boundary energy density is specified at a position $\mathbf{r} \in \Gamma_f$, where Γ_f is the boundary of Ω_f, and with tangential slowness $\mathbf{p}_r = [\sin(\theta)/c_0 \;\; \phi]^T$ for direction coordinates $\theta \in [0, \pi/2)$ and $\phi \in [0, 2\pi)$ as shown in Fig. 1. Note that we consider the case where the fluid boundary Γ_f coincides with the entire structure Ω_s, which forms a global interface. In order to relate ρ_A and ρ_V on the structure Ω_s, we introduce the following mappings:

$$m_{\mathbf{r}} : \phi \to (s, \gamma). \tag{13}$$

Here $m_{\mathbf{r}}$ maps the angle $\phi \in [0, 2\pi)$ at a point $\mathbf{r} \in \Omega_s$ described above to the associated position $s \in \Gamma_s$ and direction γ at $s \in \Gamma_s$ pointing towards $\mathbf{r}$, see Fig. 1. This mapping is invertible in convex domains[1], which we assume from hereon for simplicity. For clarity, will write $m_{\mathbf{r}}$ out fully in the form

$$m_{\mathbf{r}}(\phi) := (\sigma_{\mathbf{r}}(\phi), \psi_{\mathbf{r}}(\phi)) = (s, \gamma). \tag{14}$$

The directionality relationship (10) and the invertibility of the mapping (13) lead to an expression for $\mathbf{p}_r$ in the form

$$\mathbf{p}_r = \begin{bmatrix} \dfrac{\sqrt{c_b^2 - c_0^2}}{c_0 c_b} & \phi \end{bmatrix}^T = \begin{bmatrix} \dfrac{\sqrt{c_b^2 - c_0^2}}{c_0 c_b} & m_{\mathbf{r}}^{-1}(s, \gamma) \end{bmatrix}^T.$$

Imposing the energy relationship (7) at each point on the surface of the plate Ω_s and for each direction specified by (k_x, k_y), the following phase-space energy coupling relationship may then be derived for $k_b < k_0$:

$$\rho_V\left(\mathbf{r}, c_0^{-1} c_b^{-1} \sqrt{c_b^2 - c_0^2}, \phi\right) = \frac{\rho_f k_0^2}{\rho_s h (k_0^2 - k_b^2)} \rho_A(\sigma_{\mathbf{r}}(\phi), \sin(\psi_{\mathbf{r}}(\phi))/c_b), \quad \forall \mathbf{r} \in \Omega_s, \tag{15}$$

which specifies the radiation into Ω_f for the energy density ρ_A. By reciprocity we may also rearrange (15) to express the fluid loading on the structure due to ρ_V in the form

$$\rho_A(\varphi(s, p_s); \mathbf{r}) = \frac{\rho_s h (k_0^2 - k_b^2)}{\rho_f k_0^2} \rho_V\left(\mathbf{r}, c_0^{-1} c_b^{-1} \sqrt{c_b^2 - c_0^2}, m_{\mathbf{r}}^{-1}(s, \gamma)\right), \quad \forall \mathbf{r} \in \Omega_s. \tag{16}$$

The boundary map φ has been applied on the left to reflect the fact that here we are specifying the flow from the volume into the structure, and thus into the structural mesh cell boundaries. Note that the coupling relationship (15) is defined for a fixed directions θ. In order to apply a discretisation and approximate the boundary densities using orthogonal polynomial

[1] More precisely, $m_{\mathbf{r}}$ is invertible provided that Ω_s is starlike with respect to the point $\mathbf{r}$.

basis expansions, it will be necessary to move the directional dependence to the right hand side and rewrite the relation (15) as

$$\rho_V(\mathbf{r},\mathbf{p}_r) = \frac{\rho_f k_0^2}{\rho_s h(k_0^2-k_b^2)} \frac{c_0\delta\left(c_0^{-1}\left(\sin\theta - c_b^{-1}\sqrt{c_b^2-c_0^2}\right)\right)}{\sin\theta} \rho_A(\sigma_{\mathbf{r}}(\phi), \sin(\psi_{\mathbf{r}}(\phi))/c_b). \tag{17}$$

Here the delta distribution in (17) specifies the direction $\theta = \arccos(k_b/k_0)$. Finally, note that the relationship (16) is specified with reference to a fixed position $\mathbf{r} \in \Omega_s$. We actually require that the density is specified on the boundary Γ_s. This means that we must effectively treat each $\mathbf{r} \in \Omega_s$ that reaches (s,γ) under the action of the map $m_{\mathbf{r}}$ as a source point illuminating the boundary phase-space coordinate leading to

$$\rho_A(\varphi(s,p_s)) = \frac{\rho_s h(k_0^2-k_b^2)}{\rho_f k_0^2} \int_{\Omega_s} \delta(\gamma - \psi_{\mathbf{r}}(\phi)) \rho_V\left(\mathbf{r}, c_0^{-1}c_b^{-1}\sqrt{c_b^2-c_0^2}, m_{\mathbf{r}}^{-1}(s,\gamma)\right) \mathrm{d}\mathbf{r}. \tag{18}$$

The delta distribution here fixes the points $\mathbf{r}$ along the trajectory starting at (s,p_s) with direction γ.

6. Conclusions and further work

In this paper we have discussed the coupling of phase-space densities in two- and three-dimensions in order to apply DFM to the fluid-structure interaction problem of a vibrating elastic structure coupled to a fluid volume. By considering the sound radiated by a time-harmonic bending wave above the critical frequency, we have derived energy and directionality relationships between the fluid and the structure in the high frequency regime. Based on these relationships, we have detailed a set of coupling relations for the two- and three-dimensional boundary phase space densities of DFM on the global interface between the fluid and the structure. This paper has therefore provided a theoretical background for coupling phase-space densities in two- and three-dimensional domains, leading to a set of relations that may be discretised and investigated numerically in future work.

Acknowledgements

Support from the EU (FP7-PEOPLE-2013-IAPP grant no. 612237 (MHiVec)) and the EPSRC (grant EP/M027201/1) is gratefully acknowledged.

References

[1] Sestieri A and Carcaterra A 2013 *Mech. Syst. Signal Proc.* **34** 1–18
[2] Tanner G 2009 *J. Sound. Vib.* **320** 1023–1038
[3] Chappell D J, Giani S and Tanner G 2011 *J. Acoust. Soc. Am.* **130** 1420–1429
[4] Chappell D J, Tanner G and Giani S 2012 *J. Comp. Phys.* **231** 6181–6191
[5] Lyon R H and DeJong R G 1995 *Theory and Application of Statistical Energy Analysis* (Butterworth-Heinemann)
[6] Lyon R H 1969 *J. Acoust. Soc. Am.* **45** 545–565
[7] Craik R J M 1996 *Sound Transmission through Buildings using Statistical Energy Analysis* (Gower)
[8] Glasser A S 1989 *An Introduction to Ray Tracing* (Academic Press)
[9] Kuttruff H 2000 *Room Acoustics* (Spon)
[10] Cerveny V 2001 *Seismic Ray Theory* (Cambridge University Press)
[11] Chappell D J, Tanner G, Löchel D and Søndergaard N 2013 *Proc. R. Soc. A* **469** 20130153
[12] Chappell D J, Löchel D, Søndergaard N and Tanner G 2014 *Wave Motion* **51** 589–597
[13] Bajars J, Chappell D J, Søndergaard N and Tanner G 2016 Submitted
[14] Cremer L, Heckl M and Petersson B A T 2005 *Structure-Borne Sound: Structural Vibrations and Sound Radiation at Audio Frequencies* (Springer-Verlag)
[15] Rossing T 2007 *Springer Handbook of Acoustics* (Springer Science and Business Media)

[16] Tanner G and Søndergaard N 2007 *J. Phys. A: Math* **40** R443
[17] Chappell D J and Tanner G 2013 *J. Comp. Phys.* **234** 487–498
[18] Bajars J, Chappell D J, Hartmann T and Tanner G 2016 Submitted
[19] Chappell D J and Tanner G 2014 *Chaos* **24** 043137